Disassembly time of deuterium-cluster-fusion plasma irradiated by an intense laser pulse

W. Bang

Disassembly time of deuterium-cluster-fusion plasma irradiated by an intense laser pulse

W. Bang[a)]

Los Alamos National Laboratory, Los Alamos, NM, 87544, USA

Abstract

Energetic deuterium ions from large deuterium clusters (>10 nm diameter) irradiated by an intense laser pulse ($>10^{16}$ W/cm^2) produce DD fusion neutrons for a time interval determined by the geometry of the resulting fusion plasma. We present an analytical solution of this time interval, the plasma disassembly time, for deuterium plasmas that are cylindrical in shape. Assuming a symmetrically expanding deuterium plasma, we calculate the expected fusion neutron yield and compare with an independent calculation of the yield using the concept of a finite confinement time at a fixed plasma density. The calculated neutron yields agree quantitatively with the available experimental data. Our one-dimensional simulations indicate that one could expect a ten-fold increase in total neutron yield by magnetically confining a 10 keV deuterium fusion plasma for 10 ns.

Author to whom correspondence should be addressed. Electronic mail:
[a)] wbang@lanl.gov.

I. Introduction

Numerous studies have considered the dynamics of laser-cluster-fusion reactions [1-13], and the explosion dynamics of individual clusters have been rigorously examined both theoretically and experimentally [14-22]. Although less attention has been paid to the study of the disassembly time of the plasma, an attempt had been made to measure the fusion burn time [23]. Collectively, these studies have expanded our knowledge of the details of laser-cluster-fusion experiments and have motivated the evolution of models of laser-cluster-fusion.

In Ref. [23], Zweiback *et al.* measured the fusion burn time using neutron time-of-flight detectors with thin plastic scintillators. Not having an evolved fusion yield model as we have now [24-26], their simulation predicted a fusion burn time of less than 100 ps, clearly at odds with their measured burn time of ~500 ps. Given the proper selection and preparation of their neutron diagnostics, this is too big of an error, which needs to be addressed in order to validate the current laser-cluster-fusion yield model. While they attribute the discrepancy to the insufficient time resolution of their neutron detectors [23], our simulations performed under the reported experimental conditions suggest that their measurements were likely to be accurate enough and explain where the discrepancy originates.

In previous theoretical and experimental works regarding laser-cluster-fusion experiments, it has been proposed that the disassembly time of the resulting fusion plasma would be on the order of $r_0/\langle v \rangle$ [1,2,12,17,19,27], where r_0 is the initial radius of the plasma (= approximately equal to the radius of the incident intense ($>10^{16}$ W/cm^2) laser beam on the cluster jet) and $\langle v \rangle$ is the mean speed of the energetic deuterium ions within the fusion plasma. In this article, we examine the validity of this assumption by applying a more realistic fusion yield model, one in which the number density of energetic deuterium ions drops as the cylindrical fusion plasma expands in time. We show that one can derive an analytical solution of the disassembly time, or the confinement time, which results in the same expected fusion neutron

yield assuming a constant number density of energetic deuterium ions. We also show the comparison between the predictions of our model and the available experimental data.

II. Laser-cluster-fusion model

In laser-cluster-fusion experiments using deuterium gas (or, alternatively, using deuterated methane gas), intense ($>10^{16}$ W/cm^2) ultrashort laser pulses irradiate the target, deuterium clusters. Deuterium clusters are 1–10 nm radius aggregates of deuterium molecules, bound at liquid density by van der Waals forces. These clusters are produced by forcing cold (80–100 K) deuterium gas under high backing pressure (~50 bar) through a supersonic nozzle into a vacuum [28]. If the incident laser field is sufficiently intense [29,30], the laser-cluster interaction leads to an explosion of the individual clusters generating energetic deuterium ions. The resulting deuterium fusion plasma is intrinsically cylindrical in geometric shape [29] because the incident focused laser beam is usually round and the laser pulse energy is not depleted until it propagates several mm within the cluster jet at an average atomic number density of 10^{18}–10^{19} cm^{-3}.

The so-called Coulomb explosion model has been successful in explaining how and how much the ions gain energy from the laser pulse, and has shown both qualitative and quantitative agreement with experiments [1,2,5,7,8,30]. According to this model, the electrons in a deuterium cluster first absorb the laser pulse energy as the atoms are ionized. These electrons further absorb the laser pulse energy through several absorption mechanisms [14], and escape from the cluster on a time scale short compared with the ion motion. Consequently, the highly charged clusters of deuterium ions at liquid density promptly explode by Coulomb repulsion, creating a hot (multi-keV) deuterium plasma.

The resultant deuterium ions are so energetic that they generate nuclear fusion reactions as they collide with each other within the plasma (beam-beam contribution). Nuclear fusion can also occur when the energetic deuterium ions collide with cold deuterium atoms or ions in the background cluster jet outside of the hot plasma (beam-target contribution) [6]. These fusion reactions produce a burst of 2.45 MeV neutrons from D(d, ^{3}He)n reaction and 3.02 MeV protons from the D(d, t)p reaction, whose pulse duration is determined by the geometric shape and size of the hot deuterium fusion plasma. The expected total fusion neutron yield can be expressed as [19,29]

$$Y \approx \frac{t_d}{2} \int n_D^2 <\sigma_{D(d, \,^3He)n} v>_{kT} dV + N_{ion} \int n_D <\sigma_{D(d, \,^3He)n}>_{kT/2} dl, \qquad (1)$$

where t_d is the disassembly time of the fusion plasma, n_D is the number density of deuterium ions, $<\sigma_{D(d, \,^3He)n} v>_{kT}$ is the fusion reactivity for the D(d, ^{3}He)n reaction at an ion temperature of kT defined as two thirds of the average kinetic energy of the hot deuterium ions [29], dV is the volume element of the fusion plasma, N_{ion} is the total number of energetic deuterium ions, $<\sigma_{D(d, \,^3He)n}>_{kT/2}$ approximates the velocity-averaged D(d, ^{3}He)n fusion cross-section between hot ions in the plasma and cold atoms or ions in the background cluster jet, and dl indicates integration over the dimension of the cluster jet.

The first term in Eq. (1) represents the beam-beam contribution, with the integration over the volume of the plasma, while the second term represents the beam-target contribution, with the integration over the length, l, of the cluster jet, where l varies from the initial radius of the cylindrical plasma, r_0, to the radius of the cluster jet, R. Given the near-Maxwellian velocity distribution of the hot ions observed experimentally [19,29], one can calculate the fusion reactivity and the velocity-averaged fusion cross-section using the known DD fusion cross-sections [31]. The velocity-averaged fusion cross-section is evaluated at $kT/2$ because the energy distribution of the hot ions is well fit by a Maxwellian with a temperature of kT and the cold background atoms or ions can be considered stationary.

III. Disassembly time of the plasma

The beam-beam contribution in Eq. (1) can be rewritten as

$$Y_{bb} \approx \frac{1}{2} \iint n_D(\vec{x},t)^2 < \sigma_{D(d,\,^3He)n} v >_{kT(\vec{x},t)} dVdt, \tag{2}$$

where the number density of the energetic deuterium ions within the plasma, $n_D(\vec{x},t)$, is no longer assumed to be a fixed value in time, and becomes smaller as the plasma expands in time. In this section, we aim to evaluate Eq. (2) with several assumptions and find an analytical solution for the disassembly time of the plasma.

Figure 1 shows our model for the cylindrical fusion plasma at time t, where its radius increases as a function of time as $r(t)= r_0 + <v>t$, and its length is expressed as $L(t)=L_0 + 2<v>t$ with L_0 being the initial length of the cylindrical plasma at $t=0$. We further assume that the fusion plasma is spatially homogeneous, and $n_D(\vec{x},t)$ and $kT(\vec{x},t)$ are functions of time only. Then, the average number density of energetic deuterium ions within the plasma at time t becomes $n_D(t)= N_{ion}/V(t)$, where the volume of the cylindrical plasma at time t is $V(t)=\pi r(t)^2 L(t)$. Note that N_{ion} remains nearly constant in time, and can be written as

$$N_{ion} = \int n_D(t)dV. \tag{3}$$

Therefore, within the homogeneous cylindrical plasma, Eq. (2) is simplified as

$$Y_{bb} \approx \frac{N_{ion}}{2} \int n_D(t) < \sigma_{D(d,\,^3He)n} v >_{kT(t)} dt, \tag{2a}$$

where $kT(t)$ is the average temperature of the fusion plasma at time t. As the plasma expands in time, the hot ions encounter cold background atoms and ions and transfer some of their kinetic energy to the cold background. This energy transfer causes a drop in $kT(t)$ as the plasma expands in time, which can be estimated by calculating the stopping powers with a Monte Carlo simulation code, SRIM [32,33]. In laser-cluster-fusion experiments where the overall density is that of a gas (average atomic number density of 10^{18}–10^{19} cm^{-3}), these energy losses are usually

small (~5% in Ref. [25]). Unless the gas jet density is particularly high, one can assume that $kT(t)$ remains nearly constant in time. This assumption further simplifies Eq. (2a), and the beam-beam contribution can be approximated as

$$Y_{bb} \approx \frac{N_{ion}}{2} < \sigma_{D(d, {}^3He)n} v >_{kT} \int \frac{N_{ion}}{\pi r(t)^2 L(t)} dt, \tag{2b}$$

where $n_D(t) = N_{ion}/\pi r(t)^2 L(t)$ was used. Inserting the expressions for $r(t)$ and $L(t)$, Eq. (2b) becomes an explicit function of time,

$$Y_{bb} \approx \frac{N_{ion}^2}{2\pi} < \sigma_{D(d, {}^3He)n} v >_{kT} \int_0^\infty \frac{1}{(r_0 + <v>t)^2 (L_0 + 2<v>t)} dt, \tag{2c}$$

where the total yield is calculated integrating from $t=0$ to ∞.

For $L_0 \neq 2r_0$,

$$\int_0^\infty \frac{1}{(r_0 + <v>t)^2 (L_0 + 2<v>t)} dt = \int_0^\infty [\frac{\frac{-1}{2(\frac{L_0}{2}-r_0)^2}}{(r_0 + <v>t)} + \frac{\frac{1}{L_0 - 2r_0}}{(r_0 + <v>t)^2} + \frac{\frac{1}{(\frac{L_0}{2}-r_0)^2}}{(L_0 + 2<v>t)}] dt, \tag{4}$$

and the beam-beam contribution is

$$Y_{bb} \approx \frac{N_{ion}^2}{2\pi} < \sigma_{D(d, {}^3He)n} v >_{kT} \frac{1}{2<v>} [\frac{1}{(\frac{L_0}{2}-r_0)r_0} - \frac{1}{(\frac{L_0}{2}-r_0)^2} \ln (\frac{L_0}{2r_0})]. \tag{2d}$$

On the other hand, for a spatially homogeneous plasma, the first term in Eq. (1) can be written as

$$\frac{t_d}{2} \int n_D^2 < \sigma_{D(d, {}^3He)n} v >_{kT} dV = \frac{t_d}{2} < \sigma_{D(d, {}^3He)n} v >_{kT} \frac{N_{ion}^2}{\pi r_0^2 L_0}, \tag{5}$$

where $n_D = N_{ion}/\pi r_0^2 L_0$ was used.

Equating Eq. (2d) and (5), we have the analytical solution for the disassembly time,

$$t_d = \frac{r_0^2 L_0}{2<v>} [\frac{1}{(\frac{L_0}{2}-r_0)r_0} - \frac{1}{(\frac{L_0}{2}-r_0)^2} \ln (\frac{L_0}{2r_0})]. \tag{6}$$

Defining the aspect ratio, $\alpha \equiv L_0/(2r_0)$ ($\neq 1$), Eq. (6) can be written as

$$t_d = \frac{r_0}{<v>}\left[\frac{\alpha}{\alpha-1} - \frac{\alpha \ln \alpha}{(\alpha-1)^2}\right] \equiv \gamma \frac{r_0}{<v>}. \tag{7}$$

Indeed, the disassembly time of the fusion plasma is on the order of $r_0/<v>$, where γ is defined as a function of the aspect ratio in Eq. (7) and ranges from 0 to 1. Figure 2 shows γ for different aspect ratios varying from 0 to 10. In the limiting case when α approaches 1 (marked as a dashed line, diameter=length), γ becomes 0.5, which is confirmed by directly integrating Eq. (2c) after substituting L_0 with $2r_0$. When α approaches infinity (thin filament cases occurring in most of the laser-cluster-fusion experiments), γ becomes 1 and the disassembly time is simply $r_0/<v>$.

The physical meaning of t_d is implicit in the two equations, Eqs. (2d) and (5), used to derive this time duration above. In Eq. (5), the number density is assumed to be constant in time, while the number density drops in Eq. (2d) as the plasma expands in time. In Eq. (5), nuclear fusion only occurs for a time duration t_d, whereas fusion occurs without any time limit in Eq. (2d). Defining the disassembly time as in Eq. (7), we find that this time duration can be considered as the confinement time during which the beam-beam nuclear fusion reactions occur at a fixed density. Although this interpretation is physically incorrect, it simplifies the calculation of the beam-beam contribution and results in the same neutron yield as long as the confinement time is defined as in Eq. (7). Note that the disassembly time defined here applies to the beam-beam contribution only, and the beam-target fusion reactions are not affected by this calculation.

IV. Comparison with available experimental data

Equation 2(c) gives the explicit analytical expression for the fusion neutron yields within the plasma at each time step. Likewise, the beam-target contribution can be calculated for each

time step using the above model. For this calculation, we consider the volume swept by the hot ions because only the hot ions that occupy the originally cold background region contribute to the fusion yield during the time interval dt. The beam-target contribution is given by

$$Y_{bt} \approx \int_0^\infty (N_{ion} \frac{V(t)-V_0}{V(t)}) n_D < \sigma_{D(d, \, ^3He)n} >_{\frac{kT(t)}{2}} < v > dt, \tag{8}$$

where $V_0 = \pi r_0^2 L_0$ is the volume of the plasma at $t=0$, and $N_{ion}(V(t)- V_0)/V(t)$ is the number of hot deuterium ions in the cold background region responsible for the beam-target fusion reactions. It is assumed that the number density of cold background gas is a fixed value in time, $\sim n_D$ [19,28,34]. If any dimension of the cylindrical plasma exceeds the size of the cluster jet, the fraction of the hot ions has to be adjusted accordingly.

Using Eqs. (2a) and (8), we perform one-dimensional (1D) simulations calculating the neutron yield as a function of time. In Fig. 3(a), we use the parameters reported in Ref. [23], and calculate the fusion yield per each 10 ps time step. For this simulation, we assume half of the laser pulse energy goes into the kinetic energy of the energetic deuterium ions, which is a valid assumption that has been studied theoretically [4,11] and has been confirmed experimentally in several laser-cluster-fusion experiments [13,29]. Thus, we obtain the following relation from the energy conservation law,

$$\frac{E_{laser}}{2} = N_{ion} \left(\frac{3}{2} kT\right) = (n_D \pi r_0^2 L_0) \left(\frac{3}{2} kT\right), \tag{9}$$

where E_{laser} is the laser pulse energy and the average kinetic energy of the ions is $3kT/2$. Ref. [23] notes that $E_{laser}=0.12$ J, $L_0=2$ mm, $kT=8$ keV, and $n_D=2\times10^{19}$ cm^{-3} from their measurements, and the extent of their cluster jet is 2 mm [1]. Instead of using the laser focal size given in Ref. [23] for r_0, we use Eq. (9) and calculate N_{ion} ($=E_{laser}/(3kT) =3.1\times10^{13}$ ions) and r_0 ($=16$ μm). This is a necessary step because the energy conservation law must be obeyed. Since the reported deuterium number density is rather high, we consider the energy loss to the cold background

8

atoms in our 1D simulations, which indicates that the average plasma temperature drops from 8 keV to 5.2 keV as the plasma expands.

Figure 3(a) clearly shows that fusion neutrons are produced beyond several hundred ps, in sharp contrast with the originally predicted fusion burn time of less than 100 ps from the 1D simulation in Ref. [23]. Figure 3(b) shows the total neutron yield (black line), the beam-beam contribution (blue line), and the beam-target contribution (red line) as a function of time from 0 to 2 ns. We find that the measured full-width-at-half-maximum (FWHM) fusion burn time of ~0.5 ns in Ref. [23] is in good agreement with our 1D simulation, where 73% of the total fusion reactions occur during the first 0.5 ns. (Note that the area within the FWHM of a Gaussian function is 76% of the total area.) The figure shows that the beam-target contribution becomes dominant after about 0.1 ns. Owing to the limited size of the cluster jet (=2 mm), the beam-target reactions stop contributing to the total fusion neutron yield after about 1.1 ns. Besides matching the measured fusion burn time, the expected total neutron yield in Fig. 3(b) also agrees with the measured neutron yield of 10^4 n/shot from the same experiment [23].

For an indirect but independent validation of the model, we performed 1D simulations using the experimental conditions reported in recent laser-cluster-fusion experiments [24,26] on the Texas Petawatt laser [35]. Then, we compared the predicted total neutron yield from our model with the experimentally measured neutron yield in Refs. [24,26]. In Ref. [24], an 18 keV deuterium plasma produced 1.9×10^7 neutrons in a single shot. The measured radius of the focal spot was $r_0=0.64$ mm, and the length of the plasma was $L_0=5$ mm. A Faraday cup measured the number of energetic deuterium ions, $N_{ion}=1.5 \times 10^{16}$ ions, assuming an isotropic emission of the ions, and the average number density of deuterium ions was calculated from the above values, $n_D=2.3 \times 10^{18}$ cm^{-3}. On this shot, 38% of the incident laser pulse energy (=172 J) went into the kinetic energy of the energetic deuterium ions ($N_{ion} \times 3kT/2 = 65$ J).

Figure 4(a) shows the neutron production rate (neutrons per 10 ps) from 0 to 1.5 ns. Obviously, the fusion neutrons are continuously produced well beyond the first 1 ns. Figure 4(b) shows the predicted total neutron yield (black line), the beam-beam contribution (blue lines), and the beam-target contribution (red line) as a function of time from 0 to 5 ns. The black line shows that neutrons are produced for about two nanoseconds under this experimental condition. The predicted total neutron yield agreed well with the measured neutron yield indicated as a horizontal dashed black line. The beam-beam contribution is dominant in this case owing to the large volume of the fusion plasma combined with a relatively low n_D.

Though Ref. [26] already showed good quantitative agreement, we continued the comparison for the rest of the shots reported in Fig. 5(b) of Ref. [26]. Instead of using $r_0/\langle v \rangle$ for the disassembly time as in Ref. [26], we used Eq. (7), which resulted in slightly better quantitative agreement with the experimental data.

V. Application of the model – magnetically confined plasma

There have been efforts to confine the deuterium-cluster-fusion plasma magnetically for a higher fusion yield [36-39]. It is estimated that a megagauss magnetic field could confine ~10 keV deuterium plasmas [36]. In this section, we assume a radially confined fusion plasma for τ. The temperature of the fusion plasma is assumed to be lower than 20 keV because 18 keV is the highest temperature observed with deuterium clusters to date [24,26]. Calculation of the classical diffusion rate indicates insignificant diffusion in the radial direction, so the diffusion effect was neglected in the simulation.

When the fusion plasma does not expand radially, the total neutron yield can be written as below since the beam-target contribution during the confinement time, τ, is minimal.

$$Y_{confined} \approx \frac{N_{ion}{}^2}{2\pi} < \sigma_{D(d, \,^3He)n} v >_{kT} \int_0^\tau \frac{1}{r_0^2 \, (L_0 + 2 < v > t)} dt, \tag{10}$$

where nuclear fusion reactions occur during the confinement time only, and the number density of deuterium ions drops as the plasma expands longitudinally in time.

Comparing Eq. (2d) and Eq. (10), we find that the neutron yield from the beam-beam fusion reactions is enhanced by the following ratio through magnetic confinement of the plasma.

$$\frac{Y_{confined}}{Y_{bb}} \approx \frac{\alpha}{\gamma} \ln\left[1 + \frac{2<v>\tau}{L_0}\right], \tag{11}$$

where α/γ is a function of the aspect ratio only, which increases monotonically with the aspect ratio as shown in Fig. 5(a). The aspect ratio, however, cannot increase indefinitely because the size of the cluster jet limits L_0 to be less than $2R$ (see Fig. 1) and the plasma has a finite volume.

Figure 5(b) shows the enhancement factor for α=10 and τ=10 ns while the temperature of the plasma varies from 0 to 20 keV. According to the plot, confining a 10 keV fusion plasma with α=10 for 10 ns results in an increase in the neutron yield from the beam-beam contribution by twenty times. Since the beam-target contribution is comparable to the beam-beam contribution in the unconfined ~10 keV plasma, one can expect a ten-fold increase in the overall neutron yield via magnetic confinement.

It is interesting to note that extending the confinement time further from 10 ns to 100 ns would only increase the neutron yield by about twice, as shown in Fig. 5(c). This is owing to the rapid drop in the number density of deuterium ions as the plasma expands freely in the longitudinal direction. Figure 5(d) shows the number density as a function of time for both the radially confined case (solid black line) and the unconfined case (solid red line) with α=10 at kT=10 keV. The red line quickly drops from the initial number density of 10^{19} cm^{-3}, and becomes practically zero after about 1 ns. Although the number density drops much slowly in the radially confined plasma, the density after the initial 10 ns is too low for efficient fusion reactions, resulting in the low yield enhancement seen in Fig. 5(c) with extending the confinement time beyond 10 ns.

The above analysis indicates that the magnetic confinement works most efficiently when one expects a large aspect ratio (filament-like plasma). Since L_0 has an upper limit of $2R$, this statement is equivalent to saying that it works best on a small-scale laser system where the laser pulse energy is small (~1 J) and the volume of the resulting fusion plasma is small. For example, a 5 mm long 18 keV fusion plasma that is radially confined for 10 ns at $n_D=2\times10^{19}$ cm^{-3} produces 8×10^6 neutrons in a single shot with a 1 J laser pulse (0.5 J going into the kinetic energy of the ions) according to our 1D simulation.

VI. Conclusions

We derived the analytical solution for the disassembly time of a symmetrically expanding cylindrical fusion plasma considering the beam-beam contribution to the neutron yield. We presented an analytical expression for the time-dependent beam-target contribution, and combined both contributions to calculate the expected fusion neutron yield as a function of time. Our 1D simulation for the neutron production rate correctly reproduced the measured fusion burn time in Ref. [23]. The expected total neutron yields from our 1D simulations were in good agreement with the experimentally measured neutron yields in Refs. [23,24,26]. Applying our model, we investigated the effectiveness of the magnetic confinement of the cluster-fusion plasma in the radial direction, and presented a simple relation showing the enhancement factor in the fusion yield from the beam-beam contribution.

Since the model presented in this article assumed a spatially homogeneous cylindrical plasma, one might expect some deviation from the model when the incident laser intensity is far from flat-top or Gaussian. In such cases, a proper numerical 2D modeling would be necessary to describe more complex interaction geometries.

Acknowledgments

References

[1]   T. Ditmire, J. Zweiback, V. P. Yanovsky, T. E. Cowan, G. Hays, and K. B. Wharton, Nature **398**, 489 (1999).
[2]   J. Zweiback, R. A. Smith, T. E. Cowan, G. Hays, K. B. Wharton, V. P. Yanovsky, and T. Ditmire, Phys. Rev. Lett. **84**, 2634 (2000).
[3]   I. Last and J. Jortner, Phys. Rev. Lett. **87**, 033401 (2001).
[4]   P. B. Parks, T. E. Cowan, R. B. Stephens, and E. M. Campbell, Phys. Rev. A **63**, 063203 (2001).
[5]   V. P. Krainov and M. B. Smirnov, Physics Reports **370**, 237 (2002).
[6]   G. Grillon *et al.*, Phys. Rev. Lett. **89**, 065005 (2002).
[7]   Y. Kishimoto, T. Masaki, and T. Tajima, Phys. Plasmas **9**, 589 (2002).
[8]   J. Zweiback *et al.*, Phys. Plasmas **9**, 3108 (2002).
[9]   K. W. Madison, P. K. Patel, M. Allen, D. Price, R. Fitzpatrick, and T. Ditmire, Phys. Rev. A **70**, 053201 (2004).
[10]   F. Peano, R. A. Fonseca, and L. O. Silva, Phys. Rev. Lett. **94**, 033401 (2005).
[11]   J. Davis, G. M. Petrov, and A. L. Velikovich, Phys. Plasmas **13**, 064501 (2006).
[12]   H. Y. Lu *et al.*, Phys. Rev. A **80**, 051201 (2009).
[13]   W. Bang, G. Dyer, H. J. Quevedo, A. C. Bernstein, E. Gaul, M. Donovan, and T. Ditmire, Phys. Rev. E **87**, 023106 (2013).
[14]   T. Ditmire, T. Donnelly, A. M. Rubenchik, R. W. Falcone, and M. D. Perry, Phys. Rev. A **53**, 3379 (1996).
[15]   M. Lezius, S. Dobosz, D. Normand, and M. Schmidt, Phys. Rev. Lett. **80**, 261 (1998).
[16]   J. Zweiback, T. Ditmire, and M. D. Perry, Phys. Rev. A **59**, R3166 (1999).
[17]   I. Last and J. Jortner, Phys. Rev. A **64**, 063201 (2001).
[18]   K. Y. Kim, I. Alexeev, E. Parra, and H. M. Milchberg, Phys. Rev. Lett. **90**, 023401 (2003).
[19]   K. W. Madison, P. K. Patel, D. Price, A. Edens, M. Allen, T. E. Cowan, J. Zweiback, and T. Ditmire, Phys. Plasmas **11**, 270 (2004).
[20]   I. Last, F. Peano, J. Jortner, and L. O. Silva, Phys. Plasmas **17**, 022702 (2010).
[21]   T. Fennel, K. H. Meiwes-Broer, J. Tiggesbaumker, P. G. Reinhard, P. M. Dinh, and E. Suraud, Reviews of Modern Physics **82**, 1793 (2010).
[22]   C. Peltz, C. Varin, T. Brabec, and T. Fennel, Phys. Rev. Lett. **113**, 133401 (2014).
[23]   J. Zweiback *et al.*, Phys. Rev. Lett. **85**, 3640 (2000).
[24]   W. Bang *et al.*, Phys. Rev. Lett. **111**, 055002 (2013).
[25]   M. Barbui *et al.*, Phys. Rev. Lett. **111**, 082502 (2013).
[26]   W. Bang *et al.*, Phys. Rev. E **88**, 033108 (2013).

[27]   H. Zhang *et al.*, Applied Physics Express **7**, 026401 (2014).
[28]   W. Bang *et al.*, Phys. Rev. E **90**, 063109 (2014).
[29]   W. Bang, G. Dyer, H. J. Quevedo, A. C. Bernstein, E. Gaul, J. Rougk, F. Aymond, M. E. Donovan, and T. Ditmire, Phys. Plasmas **20**, 093104 (2013).
[30]   H. Li, J. Liu, C. Wang, G. Ni, R. Li, and Z. Xu, Phys. Rev. A **74**, 023201 (2006).
[31]   H. S. Bosch and G. M. Hale, Nucl. Fusion **32**, 611 (1992).
[32]   J. F. Ziegler, M. D. Ziegler, and J. P. Biersack, Nucl. Instrum. Methods Phys. Res. B **268**, 1818 (2010).
[33]   H. Paul and D. Sánchez-Parcerisa, Nucl. Instrum. Methods Phys. Res. B **312**, 110 (2013).
[34]   D. G. Jang, Y. S. You, H. M. Milchberg, H. Suk, and K. Y. Kim, Appl. Phys. Lett. **105**, 021906 (2014).
[35]   E. W. Gaul *et al.*, Appl. Opt. **49**, 1676 (2010).
[36]   M. Wisher, W. Bang, R. D. Bengtson, S. M. Lewis, M. McCormick, H. J. Quevedo, and K. W. Struve, MEGAGAUSS, 2012 14th International Conference on Megagauss, 1 (2012).
[37]   S. Fujioka *et al.*, Sci. Rep. **3**, 1170 (2013).
[38]   J. Santos *et al.*, arXiv:1503.00247 (2015).
[39]   P. Korneev, E. d'Humières, and V. Tikhonchuk, Phys. Rev. E **91**, 043107 (2015).
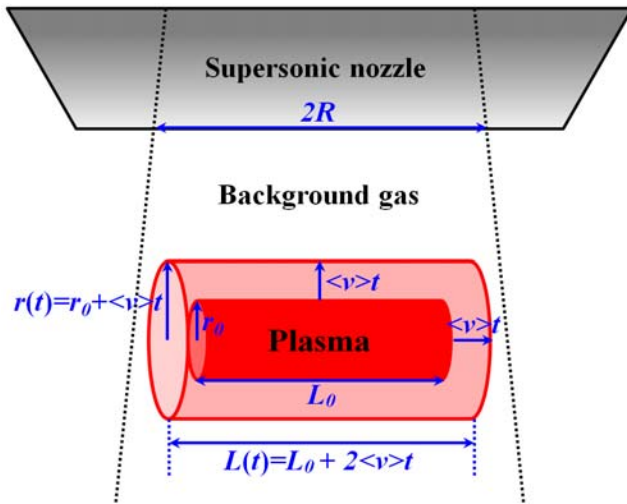
Figures

FIG. 1. (Color online) Symmetrically expanding cylindrical fusion plasma model. The cylindrical deuterium plasma with an initial radius r_0 ($\approx$ radius of the incident intense ($>10^{16}$ W/cm^2) laser beam) and length L_0 expands symmetrically in every direction at a speed $\langle v \rangle$ determined by the plasma temperature. The geometric shape of the expanded plasma at time t is approximated as cylindrical although the edges are smoothed out in time. The exit diameter ($2R$) of the supersonic nozzle limits the initial size of the plasma.
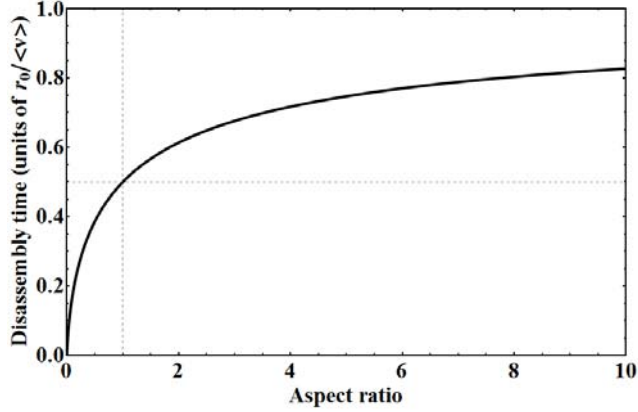
FIG. 2. The disassembly time of the cylindrical plasma in units of $r_0/{<}v{>}$, or γ, as a function of the aspect ratio defined as $L_0/(2r_0)$. The dashed lines show that the disassembly time is $0.5{\times}r_0/{<}v{>}$ when the aspect ratio is 1.
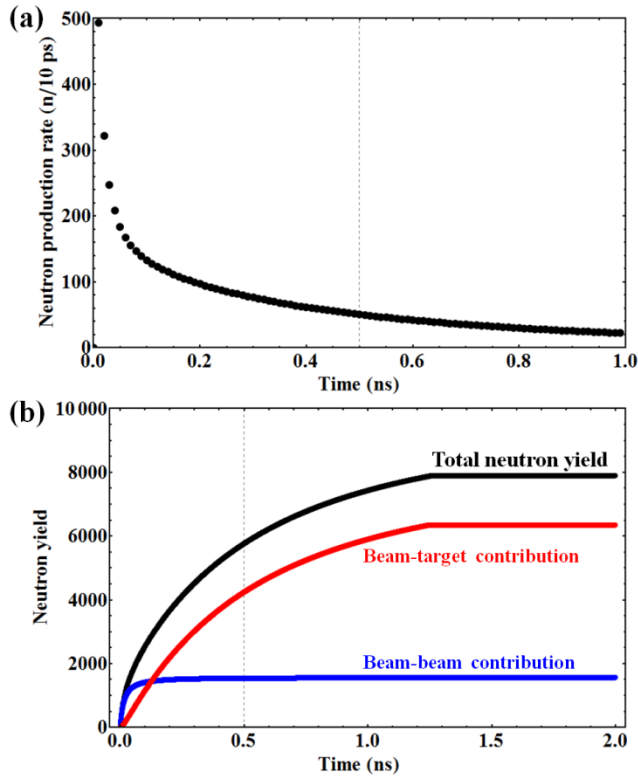

FIG. 3. (Color online) (a) Neutron production rate (number of neutrons produced during 10 ps intervals, indicated as solid black circles) as a function of time from 0 to 1 ns. A dashed line at 0.5 ns indicates the measured fusion burn time (FWHM) in Ref. [23] under the same experimental conditions. (b) The total neutron yield (black line), the beam-target contribution (red line), and the beam-beam contribution (blue line) as a function of time from 0 to 2 ns. About 73% of the total neutron yield is produced during the first 0.5 ns (indicated as a dashed line), consistent with the experimentally measured FWHM fusion burn time of ~0.5 ns in Ref. [23].
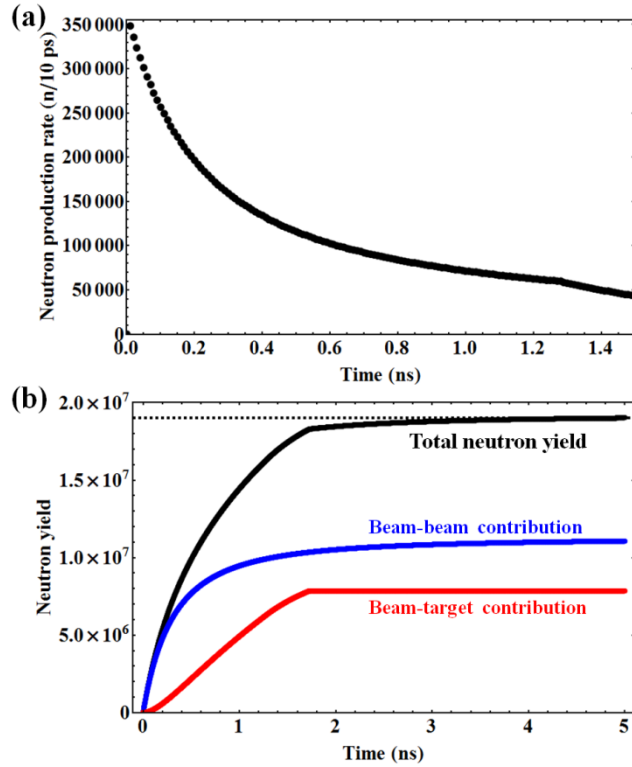
15

FIG. 4. (Color online) (a) Neutron production rate (neutrons per 10 ps, indicated as solid black circles) as a function of time from 0 to 1.5 ns. (b) The total fusion neutron yield (solid black line) as a function of time from 0 to 5 ns. The solid blue line indicates the beam-beam contribution, while the solid red line indicates the beam-target contribution. The beam-beam contribution is larger than the beam-target contribution. A dashed black line is drawn to indicate the experimentally measured neutron yield of 1.9×10^7 n/shot [24,26].
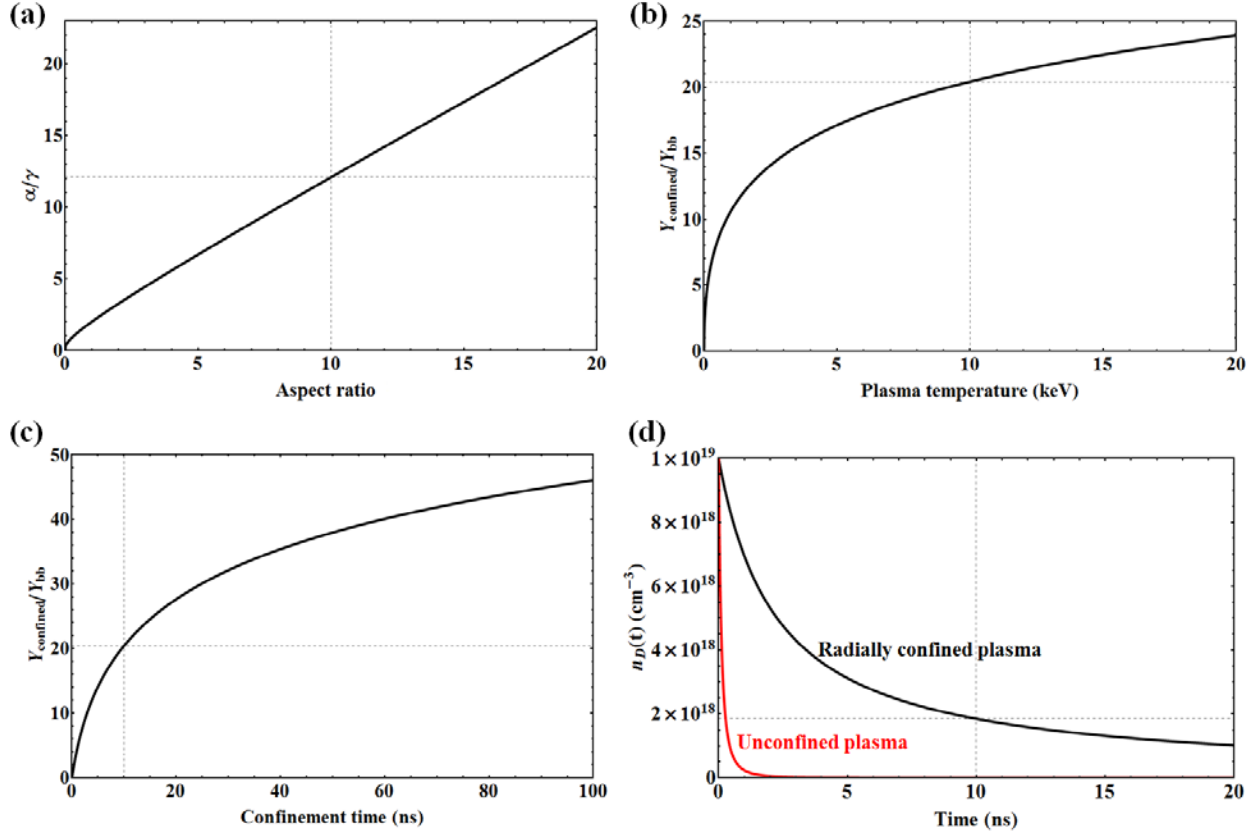
FIG. 5. (Color online) (a) α/γ as a function of the aspect ratio, α. A vertical dashed line is drawn for α=10. (b) The yield enhancement factor, $Y_{confined}/Y_{bb}$, vs. plasma temperature from 0 to 20 keV. At 10 keV (indicated as a vertical dashed line), $Y_{confined}$ is expected to be twenty times larger than the beam-beam fusion yield from an unconfined plasma. (c) The yield enhancement factor for different confinement times varying from 0 to 100 ns. A vertical dashed line is drawn for 10 ns confinement time. Note that the total neutron yield increases by about twice while the confinement time increases from 10 ns to 100 ns. (d) The number density of the energetic deuterium ions for the radially confined (solid black line) case and for the unconfined (solid red line) case.